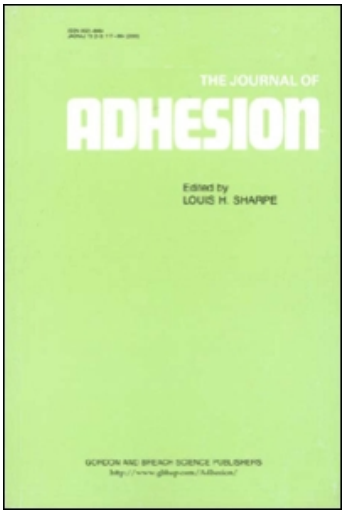

The Journal of Adhesion

Publication details, including instructions for authors and subscription information:
http://www.informaworld.com/smpp/title~content=t713453635

Effects of Film Thickness on The Work of Fracture Between Adhesives and Glass

D. A. Schupp[a]; W. W. Gerberich[a]
[a] Department of Chemical Engineering and Materials Science, University of Minnesota, Minneapolis, MN, U.S.A.

To cite this Article Schupp, D. A. and Gerberich, W. W.(1991) 'Effects of Film Thickness on The Work of Fracture Between Adhesives and Glass', The Journal of Adhesion, 35: 4, 269 — 283
To link to this Article: DOI: 10.1080/00218469108041013
URL: http://dx.doi.org/10.1080/00218469108041013

J. Adhesion, 1991, Vol. 35, pp. 269–283
Reprints available directly from the publisher
Photocopying permitted by license only

Printed in the United Kingdom

Effects of Film Thickness on The Work of Fracture Between Adhesives and Glass

D. A. SCHUPP and W. W. GERBERICH*

Department of Chemical Engineering and Materials Science, University of Minnesota, Minneapolis, MN 55455, U.S.A.

(Received March 26, 1991; in final form June 26, 1991)

In this investigation, the fracture energy of joints consisting of soda lime glass sandwiched around either an acrylate or poly(vinyl butyral) (PVB) was studied. This was accomplished for various adhesive thicknesses with the use of a tapered double cantilever beam specimen loaded in mode I. For adhesive thicknesses varying between 0.03 mm and 0.80 mm, the fracture energies ranged from 15 to 95 Pa·m for the glassy acrylate joints and from 375 to 1060 Pa·m for the more rubbery PVB joints. While the fracture energy was relatively independent of thickness for the acrylate joints, there was an increasing trend in toughness for the PVB joints. The fracture energy of the acrylate joints was modeled with a process zone model with reasonable results while the fracture energy of the PVB joints was modeled with constraints on the plastic zone. Scanning electron microscopy and measured bulk adhesive properties provided necessary input into the models.

KEY WORDS: Polymer/glass adhesion; adhesive fracture toughness; acrylate joints; PVB joints; process zone model; plastic constraint.

INTRODUCTION

Understanding adhesive failure has become critical to the optimization of many types of composite systems. Of major importance is the fracture resistance of the adhesive bond. Fracture mechanics, which can be traced to A. A. Griffith,[1,2] can provide a method to examine the fracture toughness of adhesive bonds.

The effect of adhesive thickness on bond strength has been determined by several investigators.[3–10] Most of these studies have involved epoxy or rubber-modified epoxy bonded to aluminum. This study examines a glassy acrylate and a leathery poly(vinyl butyral) bonded to a soda lime glass substrate. In addition to fracture mechanics, it involves evaluation of the fracture surface topography with a scanning electron microscope and measurements of the bulk adhesive properties.

Previous studies provided a way to estimate the thickness at which the maximum fracture energy for an adhesive joint occurs, but they did not give a quantitative approximation for the fracture energy or equations to govern the behavior of the

*Corresponding author.

fracture energy. An understanding of the effects of thickness on bond strength and possible explanations for this effect are the goals of this research.

EXPERIMENTAL

Materials

The thicknesses of two different adhesives were varied in this study. One was an acrylate consisting of acrylic acid and a silane that was supplied by Novus† in a liquid monomer form and is used to repair cracks in windshields. The other was a plasticized sheet of poly(vinyl butyral) (PVB) (Monsanto, Springfield, MA, U.S.A.) that is used in laminated safety glass in windshields. Other materials used in this study were soda lime glass slides, aluminum grips, Teflon shims, and Scotch No. 2216 B/A Clear Amber Epoxy (3M Company, St. Paul, MN, U.S.A.).

Bulk Adhesive Properties

For the bulk properties of the acrylate, it was first cast into a 127 mm × 76.2 mm × 6.35 mm mold and cured under ultraviolet (UV) light in a nitrogen environment. It was then machined into dog bone-shaped tensile specimens with a cross sectional area of 4.20 mm × 6.94 mm and a gage length of 25.4 mm. Fracture toughness was found with a disk-shaped compact tension specimen where the width was 17 mm, the thickness was 5 mm, and the original crack length was 5 mm. The toughness was then found as[11]

$$K = \frac{P}{BW^{1/2}} f(a/W) \tag{1}$$

where P is the load at failure, B is the thickness, W is the width, a is the crack length, and

$$f(a/W) = \frac{(2+a/W)}{(1-a/W)^{3/2}}\left[0.76 + 4.8\left(\frac{a}{W}\right) - 11.58\left(\frac{a}{W}\right)^2 + 11.43\left(\frac{a}{W}\right)^3 - 4.08\left(\frac{a}{W}\right)^4\right] \tag{2}$$

All tests were performed on an MTS model 810 Materials Testing System with a crosshead separation rate of 1 mm/min.

The bulk PVB was cut into dog bone-shaped tensile specimens with a cross-sectional area of 12.7 mm × 1.70 mm and a gage length of 25.4 mm. A strain offset of 0.2% was used to determine the yield stress. There was some concern as to what type of test would best represent the fracture resistance of bulk PVB. This is a material with a T_g of 28°C. Thus, it is neither a glassy polymer nor an elastomer as it is in the leathery transition range. For the form in which PVB was available, it made most sense to evaluate its bulk properties with a tear test. Trouser-leg tear test samples were used for the tear energy as calculated with a formula developed by Rivlin and Thomas,[12]

†Novus Incorporated, Minneapolis, Minnesota, U.S.A.

$$T=\frac{1}{B}(2\lambda P - W_o A_o) \tag{3}$$

where T is the tear energy, B is the thickness, λ is the extension ratio, P is the load required to tear the sample, W_o is the energy stored elastically per unit volume of the material at the time of tearing, and A_o is the cross-sectional area of the undeformed test piece. A thickness of 0.85 mm, widths of 12.7 mm and 25.4 mm, original lengths of 76.2 mm to 127 mm, and original tear lengths of 38.1 mm to 50.8 mm were used. It should be noted here that the acrylic test specimen represents a nearly opening mode I loading while the tear test is predominantly mode III.

Joint Fracture Properties

The tapered double cantilever beam (TDCB), as described by Mostovoy and Ripling,[13] was used in the study. The specimen is shown in Fig. 1 with the appropriate dimensions. This specimen has the advantage that the fracture energy is a function of only the load at failure,

$$G=\frac{4P^2}{EB^2}m \tag{4}$$

where P is the load at failure, E is the modulus of the substrate, B is the width, and m describes the taper of the beam

$$m\frac{3a^2}{h^3}+\frac{1}{h}=constant \tag{5}$$

In this study, $m=3.54$ mm^{-1}.

The assumption in using this type of specimen is that the thickness and modulus of the adhesive layer are small enough to be neglected with regard to stored elastic energy. Also, in this study, an additional 1 mm was machined off the thickness of the aluminum grips to take the thickness of the glass slides into account. The moduli of the glass and aluminum are nearly equal, minimizing the modulus mismatch

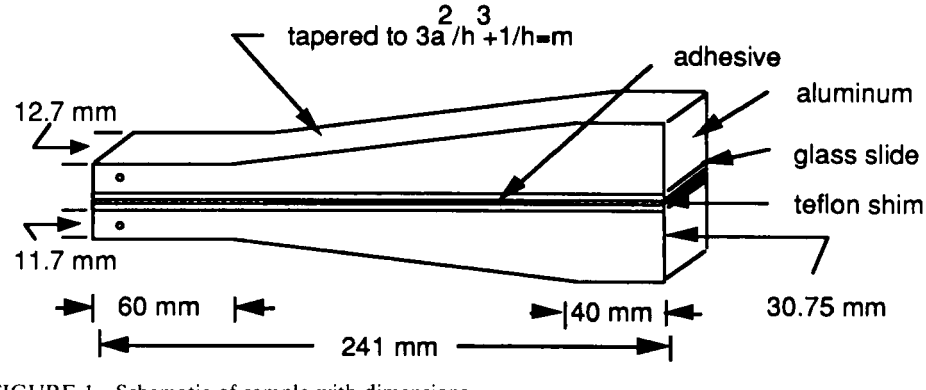

FIGURE 1 Schematic of sample with dimensions.

effect. It should also be noted that the effect of the epoxy bonding the glass to the aluminum grips was also neglected.

The glass-adhesive samples consisted of two soda lime glass slides that were 241 mm × 12.7 mm × 1 mm. Preparation consisted of cleaning with acetone to remove any surface contaminants, such as oil. Gloves were used throughout the procedure. The exact thickness of the glass slides was then measured with a Starrett 0–25 mm, 0.002 mm micrometer and recorded.

To bond the acrylate to the glass slides, Teflon shims were placed between the glass slides, and the samples were clamped together. The Teflon shims served two purposes. One, they provided a method to control the thickness of the adhesive, and two, the front shim provided a starter crack for fracture. Different thickness shims were made by compressing Teflon tape, building layers of Teflon tape, or using thicker sheets of Teflon. The thicknesses ranged from approximately 0.05 mm to 0.8 mm. Once the slides and shims were clamped together, a piece of pressure sensitive tape was placed along the bottom of the sample to form a well, or cavity. The cavity was filled with the acrylate with a disposable pipet. The entire sample was placed under a UV light for 10 minutes to cure. Afterwards, the tape and clamps were removed and both sides of the sample were carefully wiped with acetone to remove any excess acrylate. The samples were then measured to determine their final thickness and error. The adhesive thickness was determined by subtracting the thickness of the plates from the total sample thickness. Because the acrylate was initially a liquid, it easily displaced the air to remove any air bubbles. However, at larger thicknesses (greater than approximately 0.4 mm) the acrylate occasionally leaked out the bottom of the sample before curing. This made large thickness samples difficult to produce and possibly unreliable.

After the samples were made, they were attached to the aluminum grips with Scotch-Weld No. 2216 B/A Clear Amber Epoxy. Seventy-two hours after making the samples and 24 hours after attaching them to the grips, the samples were fractured on an MTS tensile testing machine, and the load-displacement data were recorded on an x-y plotter. The 72 hours allowed the acrylate to adhere fully to the glass. The fracture energy was found as described earlier.

The PVB that was received from Monsanto was plasticized. Sample making proceeded in a similar manner as the acrylate, except for the bonding procedure. As the PVB is solid at room temperature, it was cut into 241 mm × 12.7 mm strips and then placed between the two glass slides. The samples were placed into a hot press where they were pressed for 60 minutes at 143°C and 0.86 MPa. The thickness was governed by the thickness of aluminum stops placed in the press. The thicknesses were approximately 0.1 mm to 0.8 mm. Upon removal from the press, the samples were allowed to air cool. Excess PVB that was squeezed from between the glass slides was removed with a razor blade. The samples were fractured after 24 hours.

Because the PVB is initially a solid, air bubbles can easily become trapped in the sample. To help alleviate this problem, the samples were left in the press for 60 minutes instead of the original 30 minutes. Also, as the thickness decreased, fewer bubbles were present.

SEM Studies

Several fracture surfaces of representative large (0.3 mm) and small (0.05 mm) thicknesses of the acrylate were examined with a JEOL JSM-840 Scanning Electron Microscope. Sample preparations for the SEM were difficult because of the size of the vacuum chamber. To remove a sample from the fracture surface, the glass slide was placed in a vice with the aluminum grips still attached. The pressure on the sides of the slide was increased until a crack started to propagate in the glass parallel to the interface. The fracture surface was then removed from the remainder of the sample with tweezers, attached to an SEM stub, and the surface was coated with gold and carbon in an evaporator. Care was taken to ensure that the fracture surface formed during the de-adhesion process was not altered during sample preparation.

As with the acrylate, the fracture surface of the PVB-glass interface was studied with the SEM. Sample thicknesses of about 0.1 mm and 0.7 mm were prepared as described earlier.

RESULTS

Bulk Adhesive Data

The properties for both the bulk acrylate and bulk PVB are shown in Table I. The acrylate is a glassy plastic at room temperature, and the PVB is leathery. Because the acrylate is glassy and the PVB is leathery, the modulus and yield stress of the acrylate were found to be roughly 1000 and 100 times larger than the PVB, respectively, while the fracture energy of the PVB is roughly 100 times larger than the acrylate.

Joint Fracture Data

The fracture energy as a function of adhesive thickness is shown in Figures 2 and 3 for the acrylate and PVB joints, respectively.

The first adhesive system that was tested was the acrylate. The raw data points show some scatter as the thicknesses varied from 0.03 mm to 0.88 mm, and the fracture energies varied from 94.5 Pa·m to 15.1 Pa·m. The acrylate load-displacement curve displays a saw-tooth behavior. This unstable start-stop behavior results from the crack initiating, propagating a short distance, and arresting. Each individual raw data point is the average of the load peaks for that sample. When several

TABLE I
Bulk acrylate and PVB properties

Property	Acrylate	PVB
E	4000 MPa	5.9 MPa
σ_{ys}	42 MPa	0.4 MPa
K_{Ic}	1.73 MPa*m$^{1/2}$	0.59 MPa*m$^{1/2}$
G_{Ic}	.75 KPa*m	58.2 KPa*m

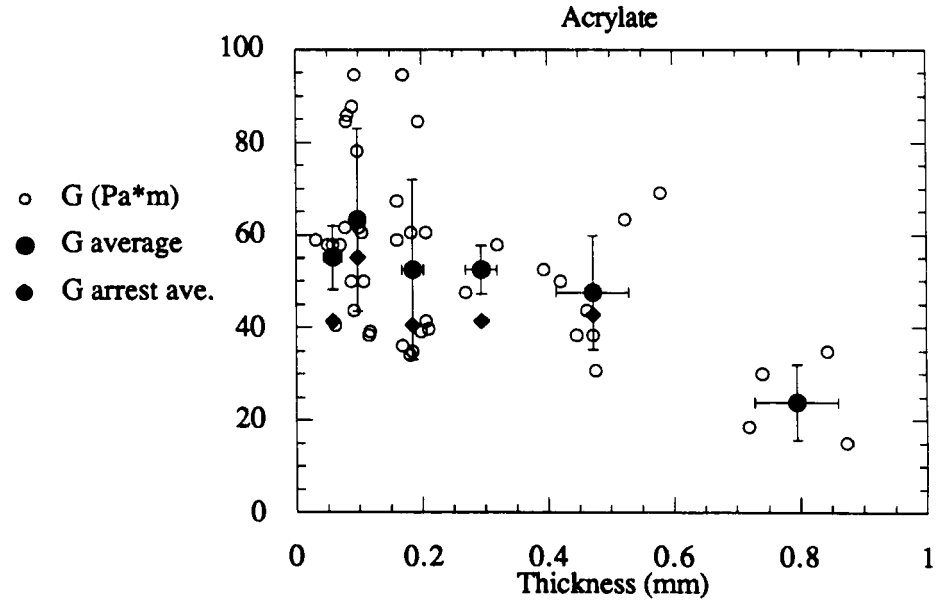

FIGURE 2 Experimental fracture energy *vs.* thickness for the acrylate.

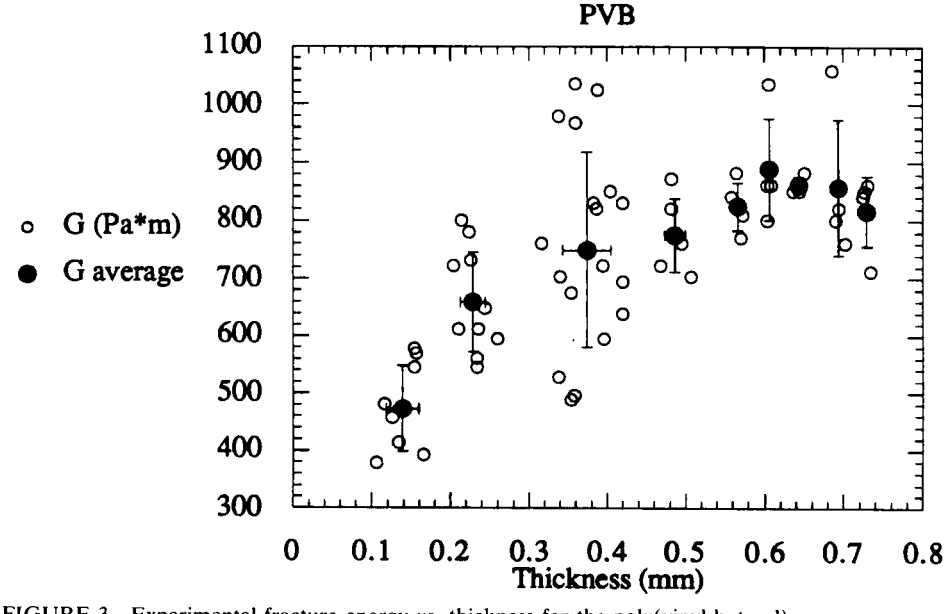

FIGURE 3 Experimental fracture energy *vs.* thickness for the poly(vinyl butyral).

data points are averaged together, the thicknesses varied from 0.06 mm to 0.80 mm, and the fracture energies varied from 63.3 Pa·m to 23.9 Pa·m. The fracture energy at crack arrest showed the same type of scatter as the fracture energy at initation and followed the same type of curve. As was stated in the experimental procedure, at large thicknesses, the acrylate occasionally leaked out of the bottom of the glass slide cavity making those measurements slightly suspect. The smaller thicknesses were bounded by the thinnest Teflon shims.

After the acrylate, the plasticized poly(vinyl butyral) was evaluated. The raw data points show less scatter than for the acrylate as the thicknesses varied from 0.10 mm to 0.74 mm, and the fracture energies varied from 378 Pa·m to 1060 Pa·m. The PVB joints showed stable crack growth, so each raw data point is the only data point taken from each joint. After averaging several data points of similar thickness together, the thicknesses varied from 0.14 mm to 0.73 mm, and the fracture energies varied from 472 Pa·m to 888 Pa·m. The limits on the thicknesses tested were the thickness of the original PVB sheet and the thickness to which the joints could be compressed at the given temperature, pressure, and time.

SEM Data

The SEM micrographs were very informative for the acrylate-glass fracture surface and are shown in Figures 4 and 5. Figure 4 shows a fiber of the acrylate with additional smaller fibrils that were presumably attached to the glass surface and stretched during the fracture process. The acrylate thickness for this sample was 0.28 mm. For a much thinner sample of 0.06 mm thickness, the fractography is shown in

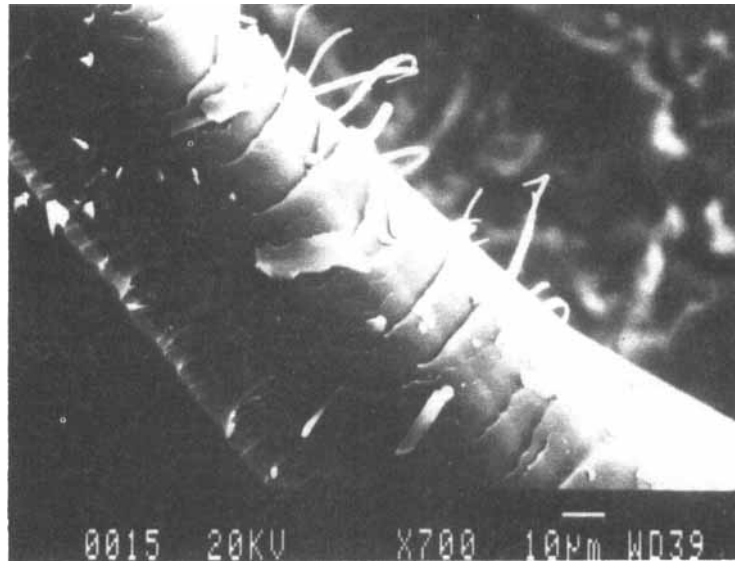

FIGURE 4 A piece of acrylate from the acrylate-glass fracture surface. Notice the smaller fibrils that were pulled out during the fracture process attached to the larger fiber.

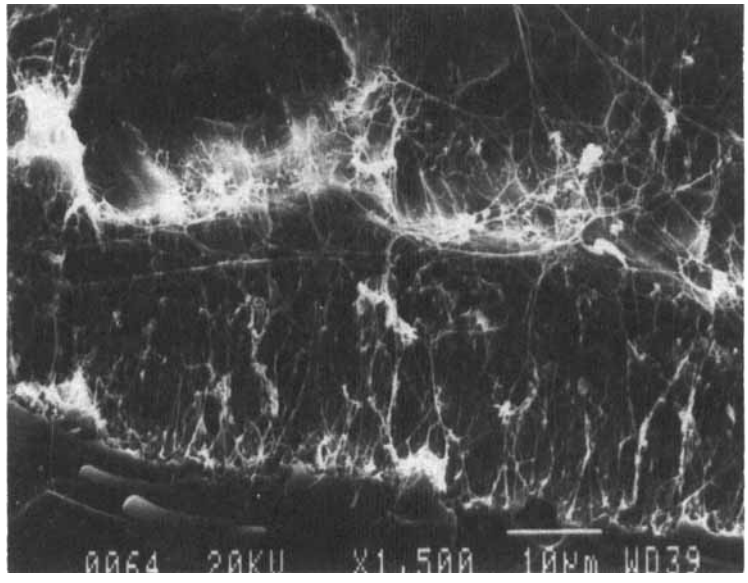

FIGURE 5 The line of fracture jumping from one glass-acrylate interface to the other. Notice the fibrils stretched between the two interfaces.

Figure 5. This shows where the line of fracture "jumped" from one glass-acrylate interface to the other. Fibrils can also be seen here.

For the PVB, the SEM micrographs were less informative than for the acrylate. They did show that the fracture seemed to be cohesive in the PVB layer, but it was *very* close to the interface. Examination with the naked eye indicated adhesive failure at the interface. At high magnification, however, a thin layer of PVB appeared to remain on the glass surface. No fibrils were seen in the micrographs. If anything, the surface appeared to consist of shallow dimples—similar to a ductile fracture surface.

DISCUSSION

Acrylate

From the fibrils visible in the micrographs and the start-stop crack growth behavior, the acrylate joint was fit to a process zone model.[14,15] In this model, the crack, a semi-cohesive zone, and the plastic zone are defined, and the stress field in each zone is integrated to obtain

$$K_I(\pi/c)^{1/2} - 2(\sigma_c - \sigma_{sc})\cos^{-1}(b/a) - 2\sigma_{sc}\cos^{-1}(c/a) = 0 . \quad (6)$$

Here σ_c is the strength of the cohesive zone, and σ_{sc} is the strength of the semi-cohesive zone. They are equal to the yield stress and the yield stress multiplied by

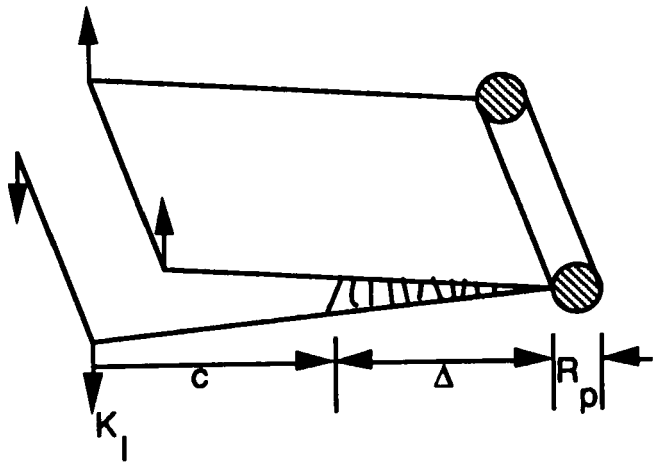

FIGURE 6 Process zone model.

the volume fraction of fibrils (f_v), respectively. Also, c is the crack length, b is the crack length plus the process zone (Δ), and a is the crack length plus the process zone plus the plastic zone diameter (R_p). A diagram of the process zone model is shown in Figure 6.

This model was used to solve for K_I, the fracture toughness. Assuming that the modulus of the system is the modulus of the acrylate, this was then converted to the fracture energy, G_I. The strengths of the cohesive and semi-cohesive zones were calculated from the results of the bulk acrylate tensile test and from the volume fraction of fibrils obtained from the micrographs, assuming a square net of fibrils. Since the exact crack length at the point of the micrograph was not known, a reasonable crack length was assumed. The process zone was determined from the change in compliance from the load-displacement curve. During loading, the load increases until the crack starts to propagate through the process zone. Eventually, the crack arrests, and a new process zone forms. By using this process, it was assumed that the crack propagated through the process zone and no further.

One final parameter remained—the plastic zone size. Unfortunately, it is a function of the fracture toughness, and that is what was being investigated. To escape a circular argument, the Dugdale-Bilby-Cottrell-Swinden (DBCS)[16,17] model was used. In it, the displacement at a position r behind the crack tip is given for a homogeneous material as[18]

$$\frac{\pi E\phi}{8(1-\nu^2)\sigma_{ys}w_I}=\frac{\phi}{\phi_{tip}}=\left(1-\frac{r}{w_I}\right)^{1/2}-\frac{r}{w_I}\ln\left[\frac{(1-r/w_I)^{1/2}+1}{(1-r/w_I)^{1/2}-1}\right]. \tag{7}$$

Here, ϕ_{tip} and ϕ are the crack opening at the crack tip and at a position r behind the crack tip while w_I is the plastic zone size. The process zone, Δ, found from the compliance change of the sample during one crack growth increment, and the length of the fibrils, found from the micrographs, were used for the values of r and ϕ,

respectively. The plastic zone and the crack tip opening displacement (CTOD) are both functions of the fracture toughness. The formulae

$$\phi_{tip} = \frac{K_I^2}{\sigma_{ys} E} \tag{8}$$

and

$$w_I = \frac{\pi}{8}\left[\frac{K_I}{\sigma_{ys}}\right]^2 \tag{9}$$

were substituted into the DBCS model for plane stress, and the fracture toughness was solved for numerically. This fracture toughness was then used to determine the plastic zone size for the process zone model, and the fracture energy of the process zone model was determined.

When solving for the plane strain case for comparison, the yield stress was set to[19]

$$\sigma_z(yield) = 3\sigma_{ys} \tag{10}$$

to take the constraint factor into account. An additional method for incorporating the thickness of the adhesive was to consider how joint thickness affected constrained yielding. Here, Orowan's[20,21] analysis of how the triaxial stress state affects the yield stress of brazed joints with respect to thickness is utilized. This gave

$$\sigma_z(yield) = \sigma_{ys}\left[1 + \frac{d}{6t}\right] \tag{11}$$

where d is the diameter of the joint (or, in this case, the width) and t is the thickness of the braze (or adhesive thickness). This puts a much larger constraint on the yield stress. The development of this formula can be seen in Lautenschlager's paper.[22] The difference is the use of either the Von Mises or Tresca criterion for yielding.

The process zone model was applied to both of the micrographs where the fibrils were observed. The results are shown in Table II. The table gives the initial data

TABLE II
Process zone predictions

Property	t = 0.28mm	t = 0.06mm
fibril length	19mm	7.9mm
f_v	2.7%	0.095%
Δ	6.2mm	2.0mm
	DBCS Model	
G (plane stress)	22.6 Pa*m	12.4 Pa*m
G (plane strain)	22.8 Pa*m	12.5 Pa*m
G (thickness constraint)	22.8 Pa*m	12.4 Pa*m
	Process Zone Model	
G (plane stress)	43.7 Pa*m	16.7 Pa*m
G (plane strain)	41.7 Pa*m	16.6 Pa*m
G (thickness constraint)	47.3 Pa*m	17.1 Pa*m

from the micrographs and load-displacement curves and the fracture energies that were predicted from both the DBCS and the process zone models.

In each case, the process zone model predicts a higher and more accurate fracture energy than the DBCS model. This is anticipated as the fibrils act as traction forces or fiber bridging which has been shown to reduce the local stress intensity for further growth. It should be emphasized here that the fibrils, which stretched across the interface from one glass surface to the adhesive, represent a cohesive failure while the vast majority of the failure appeared to be at the interface. In the final analysis, spatially-resolved spectroscopy of the glass-side would have to be accomplished to verify that this were a true interface failure as opposed to a near-interface failure. For the 0.28 mm thick sample, the process zone model gives a very good estimate of the joint fracture energy. Compared with Figure 2, the values are 47.3 Pa·m (calculated) to 55 Pa·m (experimentally determined). Using the thickness constraint proposed by Orowan gives the closest prediction, but all of the predictions are close. For the 0.06 mm thick sample, Orowan's thickness constraint still gives the best prediction, but all of the predictions are approximately a factor of three too low.

PVB

Because of the steady load-displacement curve and the lack of fibrils, the process zone model is not applicable. However, another approach may be used to predict the fracture energies. The plastic zone was assumed to be less than or equal to the thickness of the adhesive layer

$$R_p \leq t \tag{12}$$

$$R_p = t = \frac{1}{\pi}\left[\frac{K_I}{\sigma_{ys}}\right]^2 . \tag{13}$$

After setting the plastic zone equal to the thickness, the fracture energy was solved for in terms of the thickness and the yield stress since the strain energy released is the strain energy density times the volume and the release rate is per unit fracture area. This gives

$$G_I = \frac{\pi \sigma_{ys}^2}{E} t . \tag{14}$$

An assumption was made that the modulus of the system was the modulus of the PVB. This is appropriate for the resistance side of the energy balance since the PVB is absorbing the energy while the specimen, of higher modulus, is releasing elastic energy. Note that Eqs. (12–14) are appropriate for elastic-plastic materials. There is necessary cause for concern here considering that this polymer is in the leathery transition region rather than being a glassy polymer with a well-defined yield stress. Still, it was thought that the constraining effect of the glass and the relatively high strain rates at the crack tip might make this behave more glassy-like than rubbery-like during adhesive failure. Thus, for first order estimates, this elastic-plastic approach was utilized.

Differences in plane stress, plane strain, and Orowan's thickness constraint were taken into account in the value of the yield stress, as described in the previous section, Eqs. (10–11). Each of those theoretical fracture energies are shown in Figure 7 along with the experimentally determined values. An enlargement of the experimentally tested thicknesses is shown in Figure 7a while a wider range of thicknesses for theoretical comparison is shown in Figure 7b.

As can be seen, the experimentally determined values appear to be bounded by the plane strain situation and Orowan's thickness constraint. The experimentally determined values seem to follow a plane strain phenomenon (increasing fracture energy with increasing thickness) up to the maximum fracture energy. At this point, they seem to decrease, consistent with Orowan's prediction of constrained yielding. However, this representation is not meant to represent an upper and lower bound limit analysis but rather to illustrate the lack of quantitative agreement at relatively low thicknesses. Because of the uncertainties of the constraint influence and the viscoelastic nature of the PVB in largely changing the stresses in the plastic strip to well beyond the measured yield stress, it is not expected that this simple yield stress model should be adequate. This suggests that a more meaningful analysis based upon molecular motion constraint or viscoelastic dissipation is required.

Comparison with Previous Work

Previous studies[3–10] found that a maximum fracture energy occurred at a particular thickness and that this thickness was equal to the size of the plastic radius of the

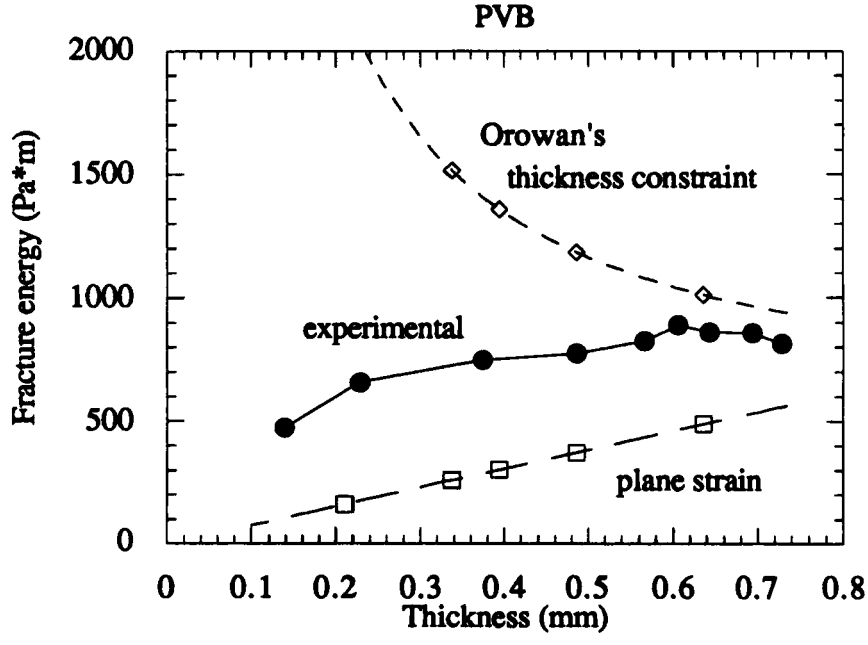

FIGURE 7a Theoretical fracture energies *vs.* thickness for experimentally tested thicknesses.

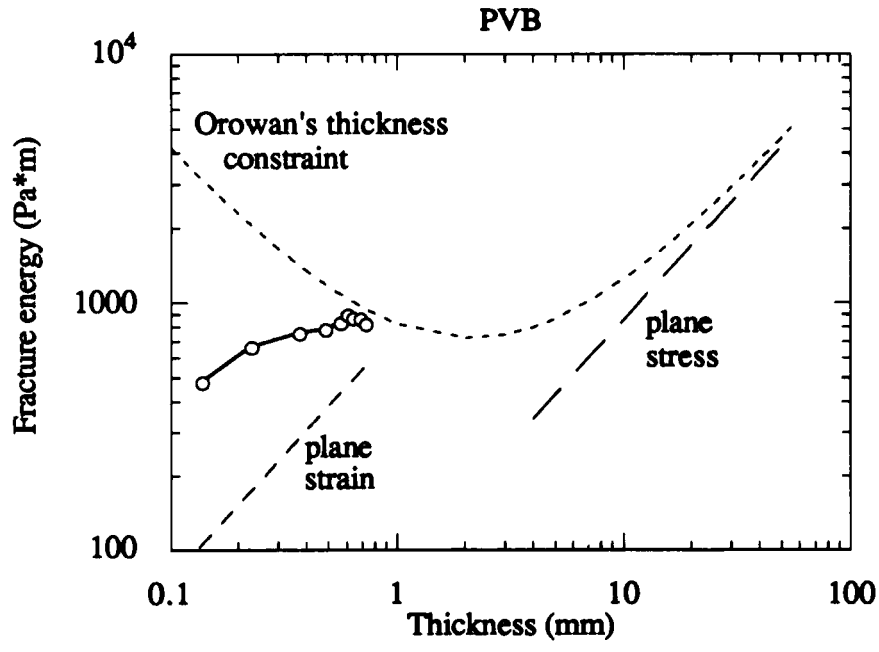

FIGURE 7b Theoretical fracture energies *vs.* thickness for a wide range of thicknesses.

bulk adhesive. This study found no statistically significant maximum fracture energy for either the acrylate or the PVB joints, although there was a plateau in the latter at 0.6 mm and greater. The plastic radii for these materials are 0.54 mm and 0.18 mm for the acrylate and 0.693 m and 0.231 m for the PVB for both the plane stress and plane strain stress states, respectively. While the thickness of the acrylate is similar to the plastic radius of the plane strain case, the PVB values are much too high to expect a maximum.

Past studies found that the fracture energy at crack arrest was fairly constant with respect to thickness, consistent with the present findings. Finally, previous studies considered predominantly cohesive failure in the center of the adhesive layer. In this study, the acrylate appeared to fail by interfacial adhesive failure while the PVB failed by cohesive failure very close to the interface. It is important in this regard to note that the ratio of the bulk to adhesive joint failure was about 15 for the acrylate and about 70 for the PVB. Compare Table I with Figures 2 and 3. Thus, even though the failure was cohesive in the latter case, the constraining influence of the substrate had more effect on the work of adhesion than the strength of the interfacial bond. That is, the ranking of the fracture resistances had little to do with the adhesion between the polymer and glass if only bond types are considered. The silane in the acrylate should form covalent bonds with the glass while the PVB should form hydrogen bonds. Based solely on bond strength, the acrylate joints should be much tougher; however, if the stresses are greater in the more glassy acrylic the singularity would give very high stresses to break the adhesive bond. In

fact, converting G values to stress intensities gives 0.45 MPa·m$^{1/2}$ and 0.068 MPa·m$^{1/2}$ for acrylate and PVB joints. From a stress distribution standpoint ($\sigma_{ij} \propto K$), the local stresses in the acrylic would be much greater. The appropriate considerations then are both the bonding and the local available stress to fracture such bonds.

SUMMARY

For the average adhesive thicknesses of this study, the viscoelastic-plastic PVB adhesive had a work of fracture near 750 Pa·m compared to 50 Pa·m for the glassy acrylate adhesive. Start-stop crack growth behavior and fibrils visible from SEM micrographs of the acrylate-glass fracture surface suggested the use of a process zone fracture toughness model that gave very reasonable fracture toughness approximations. Restrictions on the size of the plastic radius in the PVB joints provided a model which bracketed the fracture toughness results. The nonspecificity of the agreement suggests other models may be more appropriate for PVB. In the present study, it appears that the constraining influence of the joint may produce a greater influence on the work of adhesion than the interfacial fracture resistance of the bond itself.

Acknowledgments

The authors would like to thank Dr. David of Monsanto, Springfield, Massachusetts, U.S.A., and Bill Wiele of Novus Incorporated, Minneapolis, Minnesota, U.S.A. for supplying the PVB and acrylate, respectively. We would also like to acknowledge Novus Incorporated, and the NSF Sponsored Engineering Research Center for Interfacial Engineering, Grant NSF/CDR-8721551 for funding this project.

References

1. A. A. Griffith, *Phil. Trans. Roy. Soc. London A* **221,** 163 (1921).
2. A. A. Griffith, *Proc. Ist Int. Congress Appl. Mech.*, 53 (1924).
3. S. Mostovoy, E. J. Ripling, and C. F. Bersch, *J. Adhesion* **3,** 125 (1971).
4. S. Mostovoy and E. J. Ripling, *J. Appl. Polym. Sci.* **15,** 661 (1971).
5. W. D. Bascom, R. L. Cottington, R. L. Jones and P. Peyser, *J. Appl. Polym. Sci.* **19,** 2545 (1975).
6. W. D. Bascom and R. L. Cottington, *J. Adhesion* **7,** 333 (1976).
7. D. L. Hunston, J. L. Bitner, S. L. Rushford, J. Oroshnik and W. S. Rose, *J. Elast. and Plast.* **12,** 133 (1980).
8. A. J. Kinloch and S. J. Shaw, *J. Adhesion* **12,** 59 (1981).
9. H. Chai, in *Composite Materials: Testing and Design (7th Congress),* **ASTM STP 893,** J. M. Whitney, Ed. (American Society for Testing and Materials, Philadelphia, 1986), p. 209.
10. S. Mall and G. Ramamurthy, *Int. J. Adhesion and Adhesives* **9,** 33 (1989).
11. R. W. Hertzberg, *Deformation and Fracture Mechanics of Engineering Materials* (John Wiley & Sons, New York, 1989), p. 655.
12. R. S. Rivlin and A. G. Thomas, *J. Polym. Sci.* **10,** 291 (1953).
13. S. Mostovoy, P. B. Crosley and E. J. Ripley, *J. Materials* **2**(3), 661 (1967).
14. S. J. Israel, C. S. Kantamneni and W. W. Gerberich, in *Mechanical Behavior of Materials,* K. J. Miller and R. F. Smith, Eds. (Pergamon Press, New York, 1979), p. 393.
15. W. W. Gerberich, in *Fracture Mechanics: Eighteenth Symposium,* **ASTM STP 945,** D. T. Read and R. P. Reed, Eds. (American Society for Testing and Materials, Philadelphia, 1988), p. 5.
16. D. S. Dugdale, *J. Mech. Phys. Solids* **8,** 100 (1960).

17. B. A. Bilby, A. H. Cottrell and S. H. Swinden, *Proc. Roy. Soc. A* **272,** 304 (1963).
18. E. Smith, *Int. J. Fracture* **17,** 443 (1981).
19. A. U. De Koning, *Results of Calculations with TRIM 6 and TRIAX 6 Elastic-Plastic Elements,* Nat. Aerospace Inst., Amsterdam, Rept. MP73010 (1973).
20. E. Orowan, J.F. Nye and W. J. Cairns, *M.O.S. Armament Res. Dept. Rep.* **16,** 35 (1945).
21. J. J.Saxton, A. J. West and C. R. Barrett, *Met. Trans.* **2** (April), 999 (1971).
22. E. P. Lautenschlager, B. C. Marker, B. K. Moore and R. Wildes, *J. Dent. Res.* (November-December), 1361 (1974).